

Size-sensitive melting characteristics of gallium clusters: Comparison of Experiment and Theory for Ga_{17}^+ and Ga_{20}^+

Sailaja Krishnamurty, S. Chacko, and D. G. Kanhere
*Department of Physics, and Centre for Modeling and Simulation,
 University of Pune, Ganeshkhind, Pune-411 007, India*

G. A. Breaux, C. M. Neal, and M. F. Jarrold
Chemistry Department, Indiana University, 800 East Kirkwood Avenue, Bloomington, Indiana 47405-7102
 (Dated: November 17, 2018)

Experiments and simulations have been performed to examine the finite-temperature behavior of Ga_{17}^+ and Ga_{20}^+ clusters. Specific heats and average collision cross sections have been measured as a function of temperature, and the results compared to simulations performed using first principles Density-Functional Molecular-Dynamics. The experimental results show that while Ga_{17}^+ apparently undergoes a solid-liquid transition without a significant peak in the specific-heat, Ga_{20}^+ melts with a relatively sharp peak. Our analysis of the computational results indicate a strong correlation between the ground-state geometry and the finite-temperature behavior of the cluster. If the ground-state geometry is symmetric and “ordered” the cluster is found to have a distinct peak in the specific-heat. However, if the ground-state geometry is amorphous or “disordered” the cluster melts without a peak in the specific-heat.

PACS numbers: 61.46.+w, 36.40.-c, 36.40.Cg, 36.40.Ei

I. INTRODUCTION

It is now well established that the melting points of particles with thousands of atoms decrease smoothly with decreasing particle size, due to the increase in the surface to volume ratio.^{1,2} However, unlike particles with thousands of atoms or the bulk material, probing the finite-temperature properties of small clusters (with < 500 atoms) is non-trivial and remains a challenging task. Experimental studies of the melting transitions of clusters in small size regime have only recently become possible.^{3,4,5,6,7,8,9,10,11} Several interesting phenomena have been observed, including melting temperatures that rise above the bulk value^{7,8} and strong size-dependent variations in the melting temperatures.^{9,10} These experimental findings have motivated many theoretical investigations on the finite-temperature behavior of clusters.^{12,13,14,15,16,17,18} Simulations based on first principles have been particularly successful in quantitatively explaining the factors behind the size-dependent variations in the melting behavior of clusters.¹⁷ Thus, a confluence of recent advances in experimental methods and theoretical studies using first principles methods have set the stage for a major increase in our understanding of phase transitions in these small systems.

Coming to the present work on gallium clusters, it is by now well known that gallium clusters not only melt at substantially higher temperatures than the bulk ($T_{m[\text{bulk}]} = 303$ K),⁸ but they also exhibit wide variations in the temperature dependences of their specific-heats, with some clusters showing strong peaks (due to the latent heat), while others (apparent “non-melters”) showing no peak.⁹ These features show a strong dependence on cluster size, where the addition of a single atom can change a cluster with no peak in the specific-heat into a

“magic melter” with a very distinct peak. This behavior has been observed for gallium clusters, Ga_n , with $n = 30-55$.

In the present work, we probe the melting behavior of small gallium cluster ions where we show that the “non-melting” and “melting” features in the specific-heats are observed in clusters as small as Ga_{17}^+ and Ga_{20}^+ , respectively. Prior experimental results for Ga_{17}^+ over a limited temperature range showed no evidence for a melting transition.⁸ The experimental results in this case were specific-heat measurements performed using multi-collision induced dissociation, where a peak in the specific-heat due to the latent heat was the signature of melting. On the other hand, recent simulations for Ga_{17} show a broad peak in the specific-heat centered around 600 K. The previous specific-heat measurements for Ga_{17}^+ extended only up to 700 K, so one possible explanation for this apparent discrepancy is that the melting transition occurred at a slightly higher temperature than examined in the experiments. Here, we report specific-heat measurements for Ga_{17}^+ over a more extended temperature range, along with specific-heat measurements for Ga_{20}^+ . While no peak is observed in the heat-capacities for Ga_{17}^+ , a peak is observed for Ga_{20}^+ .

To further probe the melting transitions in these clusters, ion mobility measurements were performed for Ga_{17}^+ and Ga_{20}^+ as a function of temperature. The ion mobility measurements provide average collision cross sections which can reveal information about the shape and volume changes that occur on melting. For example, a cluster with a non-spherical geometry might be expected to adopt a spherical shape (a liquid droplet) on melting. If there is not a significant shape change, there may still be a volume change on melting. Most bulk materials expand when they melt (the liquid is less dense than the

solid). Even in the absence of a significant shape or volume change, the cross sections might show an inflection at the melting transition due to the thermal coefficient of expansion of the liquid cluster being larger than for the solid (in the macroscopic regime most liquids have larger coefficients of expansion than the corresponding solids). An inflection is observed in the cross sections for both Ga_{17}^+ and Ga_{20}^+ . Thus, the ion mobility measurements suggest that Ga_{17}^+ as well as Ga_{20}^+ are in a liquidlike state above 800 K.

To explore the reasons behind the behavior outlined above (i.e., to determine why Ga_{17}^+ apparently melts without a peak in its specific-heat, while a peak is observed for Ga_{20}^+), we have carried out first principles Density-Functional (DF) Molecular-Dynamics (MD) calculations on both clusters. The ground-state structure and the bonding within the clusters is analyzed. The ionic specific-heat is computed using multiple histogram method.^{19,20} The calculated specific-heats for Ga_{17}^+ show three broad low intensity maxima that extend from 300 to 1400 K. This resembles the experiment results where the measured specific-heats are relatively featureless. In contrast, the calculated specific-heats for Ga_{20}^+ show a clear peak around 750 K. This is in excellent agreement with the peak obtained from experimental measurements (which occurs at around 700 K). Finally, our theoretical results show that the features in the specific-heat curves are influenced by the ground-state geometry, the bonding of the atoms within the ground-state structure, and the isomer distribution that becomes accessible as the temperature is raised.

In Sec. II, we present the experimental methods and the computational details. In Sec. III we discuss the experimental and theoretical results on both clusters. We conclude our results in Sec. IV.

II. METHODOLOGY

Specific-heats were measured using the recently developed multi-collision induced dissociation approach. The cluster ions are generated by laser vaporization of a liquid gallium target in a continuous flow of helium buffer gas. After exiting the laser vaporization region of the source the clusters travel through a 10 cm long temperature variable extension where their temperature is set. Cluster ions that exit the extension are focused into a quadrupole mass spectrometer where a particular cluster size is selected. The size selected clusters are then focused into a collision cell containing 1 Torr of helium. As the clusters enter the collision cell they undergo numerous collisions with the helium, each one converting a small fraction of the ions translational energy into internal energy. If the initial kinetic energy is high enough some of the cluster ions may be heated to the point where they dissociate. The dissociated and undissociated cluster ions are swept across the collision cell by a small electric field and some of them exit through a small aperture. The ions that exit

are analyzed in a second quadrupole mass spectrometer and then detected by an off-axis collision dynode and dual microchannel plates. The fraction of the ions that dissociate is determined from the mass spectrum. Measurements are performed as a function of the ions initial kinetic energy, and the initial kinetic energy required for 50% dissociation (IKE50%D) is determined from a linear regression. IKE50%D is measured as a function of the temperature of the temperature-variable extension on the source. IKE50%D decreases as the temperature is raised because hotter clusters have more internal energy, and hence less energy needs to be added in order to cause dissociation. At the melting transition a sharp decrease in IKE50%D is expected due to the latent heat. The derivative of IKE50%D with respect to temperature is approximately proportional to the specific-heat. The proportionality constant is the fraction of the clusters initial kinetic energy that is converted into internal energy, which is estimated from an impulsive collision model. A drop in the IKE50%D values due to the latent heat of a melting transition leads to a peak in the specific-heat.

Ion mobility measurements can provide information on the shape and volume changes that occur when clusters melt. For the ion mobility measurements, the collision cell is replaced by a 7.6 cm long drift tube. 50 μs pulses of cluster ions are injected into the drift tube and the drift time distribution is obtained by recording the ions arrival times at the detector with a multichannel scalar. Average collision cross sections are obtained from the drift time distributions using standard methods.²¹

All the simulations are performed using Born-Oppenheimer molecular-dynamics based on Kohn-Sham formulation of Density-Functional Theory (DFT).²² We have used Vanderbilt's ultrasoft pseudopotentials²³ within the GGA approximation, as implemented in the VASP package²⁴ for both clusters. For all calculations, we use only $4s^2$ and $4p^1$ -electrons as valence, taking the $3d$ -electrons²⁵ as a part of the ionic core. An energy cutoff of about ≈ 10 Ry is used for the plane-wave expansion of the wavefunction, with a convergence in the total energy of the order of 0.0001 eV. Cubic supercells of lengths 20 and 25 Å are used for Ga_{17}^+ and Ga_{20}^+ , respectively. For examining the finite-temperature behavior, the ionic phase space of the clusters is sampled by isokinetic MD where kinetic energy is held constant via a velocity scaling method. For both the clusters, we split the total temperature range from 100-1400 K into 15 different temperatures. We maintain the cluster at each temperature for a period of at least 90 ps, leading to total simulation times of the order of 1 ns. The resulting trajectory data were used to compute standard thermodynamic indicators as well as the ionic specific-heat, via a multihistogram technique. Details can be found in Ref. 20,26.

III. RESULTS AND DISCUSSION

Specific-heat measured for Ga_{17}^+ and Ga_{20}^+ as a function of temperature are shown in the lower half of Fig. 1. The points are the experimental values, while the dashed line is the prediction of a modified Debye model. In the case of Ga_{17}^+ , the specific-heat shown in Fig. 1 appear to gradually increase up to around 900 K. The sharp decrease in the specific-heat above 900 K is an artifact due to evaporative cooling, the spontaneous unimolecular dissociation of the cluster ions as they travel between the source extension and the collision cell. For Ga_{20}^+ , the specific-heat show a broad maximum, around 400 K wide, centered at around 725 K. The peak for Ga_{20}^+ is significantly broader than observed for larger clusters (like Ga_{39}^+ and Ga_{40}^+) where the peak was attributed to a melting transition. However, it is well known that the melting transition, and the corresponding peak in the specific-heat, becomes broader with decreasing cluster size. Thus, even though the peak in the specific-heat for Ga_{20}^+ is around 400 K wide, it is appropriate to assign it to a finite-size analog of a bulk melting transition. The center of the peak is at around 725 K, this is well above the bulk melting point (303 K). This continues a trend reported for larger cluster sizes ($n = 30\text{--}55$) where the melting temperatures are also significantly above the bulk value. The unfilled red circles in Fig. 1 show the average collision cross sections determined for Ga_{17}^+ and Ga_{20}^+ as a function of the temperature. The cross sections are expected to systematically decrease with increasing temperature because the long range attractive interactions between the cluster ion and the buffer gas atoms becomes less important, and the collisions become harder as the temperature is raised. The thick dashed red line in the figures show the expected exponential decrease in the cross sections with increasing temperature. There is an inflection in the cross sections for Ga_{20}^+ that appears to slightly precede the peak in the specific-heat for this cluster. The inflection is consistent with a melting transition where the liquid cluster has a larger coefficient of thermal expansion than the solid. There is also an inflection in the cross sections for Ga_{17}^+ . This suggests that a solid-liquid transition also occurs for Ga_{17}^+ , but without a significant peak in the specific-heat.

To understand the reason behind the different behavior observed for Ga_{17}^+ and Ga_{20}^+ , we have carried out a detailed analysis of structure and bonding in both clusters. As will become apparent from the following discussion, that the ground-state geometry and the nature of bonding plays a crucial role in determining the finite-temperature behavior of the cluster. We begin with a discussion of the ground-state geometries of cationic Ga_{17} and Ga_{20} clusters. We have obtained more than 50 distinct equilibrium geometries by quenching more than 200 structures, selected from a few high temperature MD runs, for both sizes. In Fig. 2, we show the lowest energy structure along with some low lying excited state geometries of both clusters. The lowest energy geometry

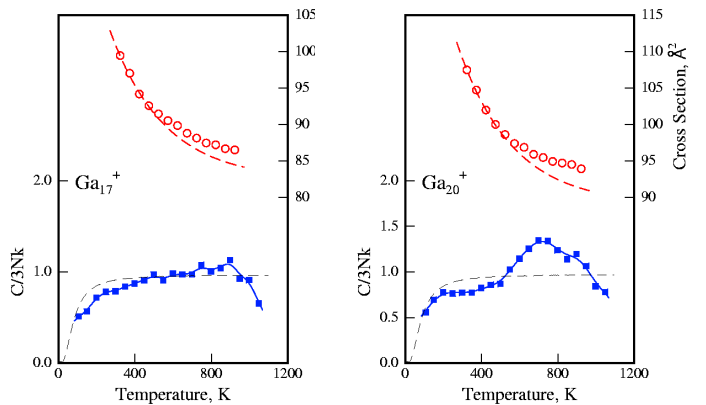


FIG. 1: Specific-heat and average collision cross sections measured for size-selected Ga_{17}^+ and Ga_{20}^+ clusters as a function of temperature. The solid blue points show the specific-heat which are normalized to $3Nk_B$ (the classical value), where k_B is the Boltzmann constant and $N = (3n - 6 + 3/2)/3$ ($n =$ number of atoms in the cluster, and $3n - 6$ and $3/2$ are due to the vibrational and rotational contributions, respectively).

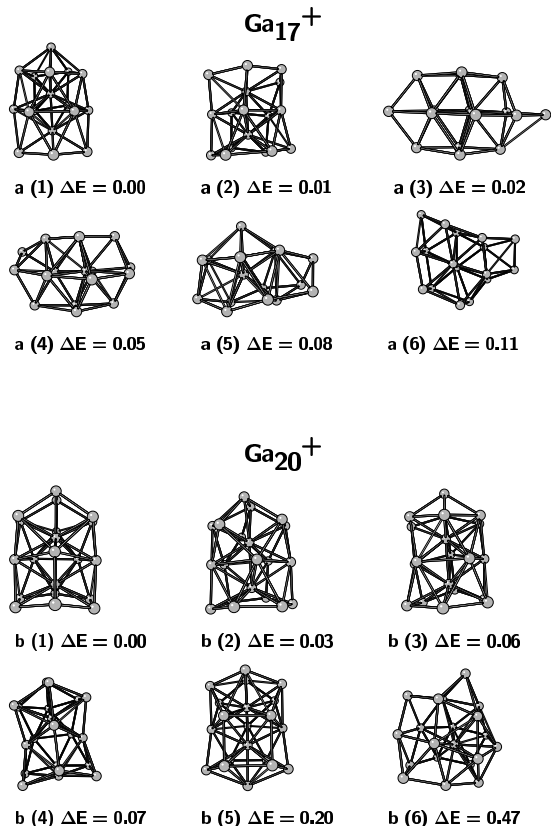


FIG. 2: The ground-state and some representative low-lying and excited-state geometries of Ga_{17}^+ and Ga_{20}^+ clusters. Fig (1) corresponds to the ground-state geometry. The energy difference ΔE is given in eV with respect to the ground-state.

of the Ga_{17}^+ cluster (see Fig. 2-a(1)) is similar to that of Ga_{17} reported in our earlier work.¹² It has a distorted decahedral structure, which suggests the possibility of further cluster growth to a 19-atom double decahedron. In contrast, the ground-state geometry of Ga_{20}^+ , shown in Fig. 2-b(1), is more symmetric. It can be described as a double decahedral structure of 19 atoms, with the bottom capped atom merging into the pentagonal plane to form a hexagonal ring. In addition, an atom from the top pentagon and the upper capped atom rearrange to accommodate the 20th atom, leading to a dome-shaped hexagonal ring.

We now analyze the structural properties in detail to get an insight into the features that influence the melting characteristics. An analysis of the bond-length distribution shows that there are 12 bonds, for each cluster, having distances less than 2.55 Å.²⁷ Interestingly, for Ga_{17}^+ , these short bonds are spread all over the cluster, whereas for Ga_{20}^+ , they form the upper and the lower hexagonal rings. The distribution of coordination numbers²⁸ indicate that for Ga_{20}^+ , almost all the atoms in the rings (about 16), have a coordination number of 4. The Ga_{17}^+ cluster, however, does not have such a uniform distribution of coordination numbers. Thus, the ground-state geometry of Ga_{17}^+ might be considered to be “disordered”, while that of Ga_{20}^+ exhibits a more-ordered structure.

Striking differences are also observed in the low energy isomers and their distribution on the potential-energy surface. As mentioned above, we have obtained more than 50 distinct isomers spanning an energy range of about 1.0 eV above the ground-states for each cluster. In Fig. 3, we plot the energies of these isomers relative to the ground-state, arranged in an ascending order. The isomers for the Ga_{17}^+ cluster appear to exhibit an almost continuous energy distribution. While a few of these isomers are severe distortions of the ground-state geometry, the rest do not show any resemblance (see Fig. 2a). It appears that for the Ga_{17}^+ isomers in this low energy regime, small rearrangements of the atoms, costing just a small amount of energy, lead to several close-lying isomers, so that the isomer distribution is almost continuous. In contrast, the isomers of Ga_{20}^+ cluster are distributed in three groups, separated by an energy gap of about 0.2 eV (Fig. 3). The first group of isomers have slightly different orientations of atoms in the hexagonal rings and are nearly degenerate with the ground-state. The second group consists of structures having only the lower hexagonal ring while the third group has no rings. This indicates that the hexagonal units of Ga_{20}^+ cluster are stable and difficult to break. The stability of the ring-pattern of Ga_{20}^+ and the isomer distribution for both clusters should have a substantial effect on the melting characteristics. Indeed, as we shall see further below, these features play a crucial role in the finite-temperature characteristics. It should be mentioned that although these observations are based on rather limited search, we believe that the general features described here are essentially correct.

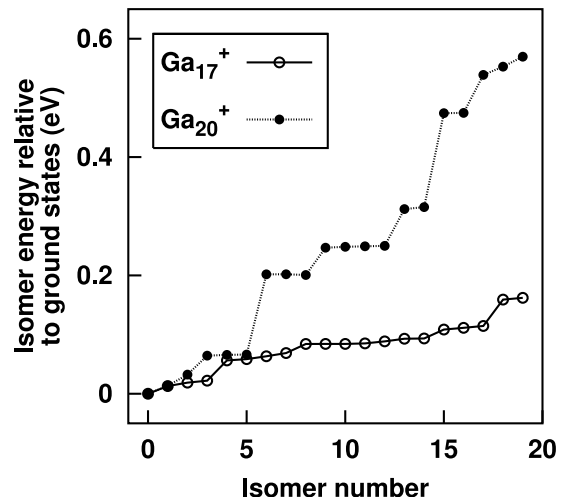


FIG. 3: The energies of the isomeric structures of Ga_{17}^+ and Ga_{20}^+ with respect to their ground-states.

TABLE I: The number of basins with more than one atom at different values of the electron localization function for the ground-state structures of Ga_{17}^+ and Ga_{20}^+ clusters. The numbers in parenthesis represent the number of atoms in each basin.

ELF value	Ga_{17}^+	Ga_{20}^+
0.85	0	1 (2)
0.77	1 (2)	2 (5,7)
0.75	3 (2,2,2)	2 (5,7)
0.73	2 (3,4)	1 (14)

The most important difference between the two clusters is the nature of the bonding. We use the concept of an electron localization function (ELF),²⁹ to describe the nature of bonding. This function is normalized to a value between zero and unity; a value of 1 represents a perfect localization of the valence charge while the value for the uniform electron gas is 1/2. The locations of maxima of this function are called *attractors*, since other points in space can be connected to them by paths of maximum gradient. The set of all such points in space that are attracted by a maximum is defined to be the *basin* of that attractor. Basin formations are usually observed as the value of the ELF is lowered from its maximum, at which there are as many basins as the number of atoms in the system. Typically, the existence of an isosurface or a basin in the bonding region between two atoms at a high ELF value, say ≥ 0.70 , signifies a localized bond in that region.

We have analyzed the electron localization functions for Ga_{17}^+ and Ga_{20}^+ clusters for values ≤ 0.85 . In Table I, we give the number of basins containing two or more atoms, for selected ELF values. The table clearly shows a fragmented growth pattern of the basins for Ga_{17}^+ , each containing very few atoms as compared to that of Ga_{20}^+ . For instance, at an isovalue of 0.75, while Ga_{17}^+ has three

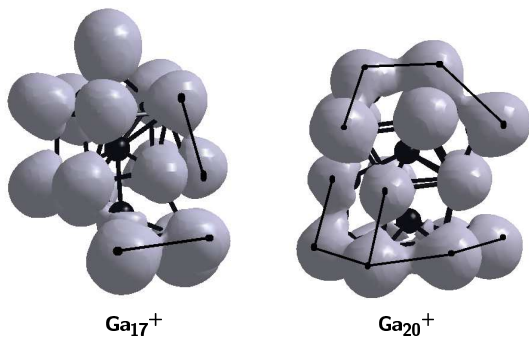


FIG. 4: The isosurface for the electron localization functions for Ga_{17}^+ and Ga_{20}^+ at an isovalue of 0.75. The black lines correspond to merged basin structures.

basins each having 2 atoms, Ga_{20}^+ has just two basins each containing 5 and 7 atoms that corresponds to the two hexagonal rings. The ELF contours for the isovalue of 0.75 are shown in Fig. 4. The merged basins structures are shown by the black lines. It may be inferred that the bonds between atoms in the hexagonal rings of Ga_{20}^+ are strong and covalent in nature with similar strengths, while the fragmented basin growth pattern in Ga_{17}^+ indicates inhomogeneity of the bond strengths.

The calculated, normalized, canonical specific-heat are shown in Fig. 5 plotted against temperature. The plot for Ga_{17}^+ exhibits a broad feature (apparently consisting of three components) which extends from 300 K to 1400 K. For Ga_{20}^+ , the calculated specific-heat remains nearly flat up to about 600 K, it then increases sharply and peaks at about 800 K, in excellent agreement with the experimental results described above. Thus, interesting size-sensitive features seen in the experimental heat-capacities are reproduced in our simulations. This behavior can be understood from our earlier discussion of the bond-length distributions, coordination numbers, isomer-distributions, and the nature of bonding in these clusters. While the Ga_{17}^+ cluster shows no real evidence for ordered behavior, the Ga_{20}^+ cluster has well-ordered ring-patterns. Thus, when Ga_{17}^+ is heated, the bonds soften gradually, and the cluster hops through all its isomers continuously. This is clearly demonstrated by the ionic motion as a function of temperature, which shows that this cluster evolves through all isomers smoothly from 300 K to 1400 K. On the other hand, the ionic motion for Ga_{20}^+ shows only minor rearrangements of the atoms until 600 K, and then the cluster visits all the isomers corresponding to the first group of isomers described above. At about 700 K, the upper hexagonal ring breaks, while at about 800 K, the lower ring breaks. Thus, melting of Ga_{20}^+ cluster is associated with the breaking of the well-ordered covalently bonded hexagonal units.

We have also analyzed the melting characteristics via traditional parameters such as, the root-mean-squared bond-length-fluctuations (δ_{rms}) and the mean-squared ionic displacements (MSD). In Fig. 6, we show the δ_{rms}

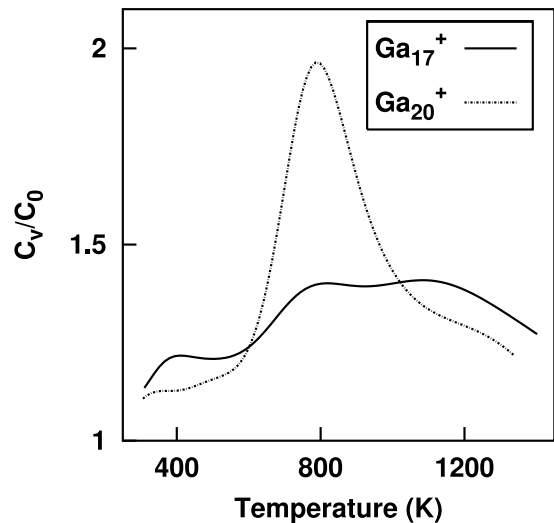


FIG. 5: Normalized canonical specific-heat for Ga_{17}^+ (continuous-line) and Ga_{20}^+ (dashed-line). $C_0 = (3n - 6 + 3/2)k_B$ is the zero temperature classical limit of the rotational plus vibrational canonical specific-heat.

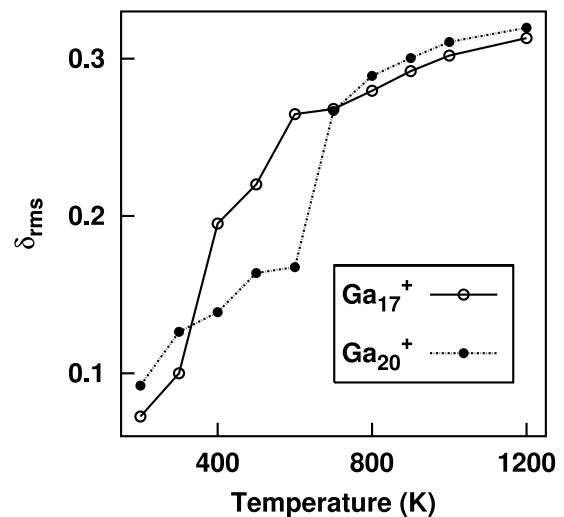


FIG. 6: Root-mean-square bond-length-fluctuations (δ_{rms}) for Ga_{17}^+ (continuous-line) and Ga_{20} (dashed-line).

for Ga_{17}^+ and Ga_{20}^+ clusters. This plot correlates well with the specific-heat curve shown in Fig. 5. The δ_{rms} for Ga_{17}^+ rises gradually from 300 K, while for Ga_{20}^+ , it rises sharply at about 700 K, and finally saturates to the same value for both clusters. It may be inferred from this observation that the behavior of both clusters at temperatures say, $T \geq 800$ K, are similar and that both clusters can be considered to be in *liquidlike* states. This conclusion is further substantiated by the MSD plots (figures not shown), which saturate at $\approx 21 \text{ \AA}^2$, at about 1200 K for both clusters.

IV. SUMMARY AND CONCLUSION

It is evident from the present study that the nature of the ground-state geometry and bonding strongly influences the finite-temperature characteristics of Ga_{17}^+ and Ga_{20}^+ . At high temperatures, $T \geq 800$ K, both Ga_{17}^+ and Ga_{20}^+ have similar root-mean-squared bond-length-fluctuations and the mean-squared ionic displacements so that both of them can be considered to be in liquidlike states. The experimental results show that while Ga_{17}^+ apparently undergoes a solid-liquid transition without a significant peak in the specific-heat, Ga_{20}^+ melts with a relatively sharp peak. The simulations show that if the cluster is “ordered” (i.e. a large fraction of the constituent atoms show similar bonding, coordination numbers, and bond energies) then it is likely to show a sharp melting transition with a significant peak in the specific-heat. On the other hand, if the cluster is “disordered” (i.e. the constituent atoms occur in a wide distribution of bonding environments) it will probably undergo a solid-liquid transition without a significant peak in the specific-heat. In the latter case, the number of isomers or conformations sampled by the cluster increases steadily as the temperature is raised, instead of the abrupt increase that occurs when a cluster undergoes a sharp melting transition.

These observations have interesting consequences for the finite-temperature behavior of small clusters as a function of cluster size. It is likely that as clusters grow in size their structures evolve from one well-ordered struc-

ture to another, passing on the way through some cluster sizes that have “disordered” structures. For instance, the 13-atom gallium cluster is predicted to have a highly symmetric decahedron structure with a bonding pattern that is similar to that found here for Ga_{20}^+ .¹² So in the present case, cluster growth from Ga_{13} (a decahedron) to (Ga_{20}^+) , a distorted double-decahedron) proceeds via a disordered Ga_{17}^+ structure. Such behavior is also observed for sodium clusters in 40 to 55 atom size range; the ground-state geometries of Na_{40} and Na_{55} are either icosahedron or close to icosahedron while that of Na_{50} has no particular symmetry.^{17,18} In such cases, we expect that the specific-heats should change from showing a well-defined peak to a rather broad one, and back again to well-defined. We believe this behavior to be generic as it has not only been observed in case of gallium clusters^{8,9} but also in case of aluminum clusters¹⁰, experimentally, and for sodium clusters in the simulations mentioned above.

V. ACKNOWLEDGMENT

The financial support of the Indo-French Center for Promotion of Advanced Research is gratefully acknowledged. C-DAC (Pune) is acknowledged for providing us with the supercomputing facilities. We gratefully acknowledge partial support of this work by the US National Science Foundation.

-
- ¹ P. Pawlow, Z. Phys. Chem. 1909, **65**, 1.
² P. R. Couchman, W. A. Jesser, Nature (London) **269**, 481 (1977).
³ M. Schmidt, R. Kusche, W. Kronmüller, B. von Issendorf, and H. Haberland, Phys. Rev. Lett. **79**, 99 (1997).
⁴ M. Schmidt, R. Kusche, B. von Issendorf, and H. Haberland, Nature (London) **393**, 238 (1998).
⁵ M. Schmidt, J. Donges, Th. Hippler, H. Haberland, Phys. Rev. Lett. **90** 103401 (2003).
⁶ H. Haberland, T. Hippler, J. Donges, O. Kostko, M. Schmidt and B. von Issendorf, Phys. Rev. Lett. **94** 035701 (2005).
⁷ A. Shvartsburg and M. F. Jarrold, Phys. Rev. Lett. **85**, 2530 (2000).
⁸ G. A. Breaux, R. C. Benirschke, T. Sugai, B. S. Kinnear, and M. F. Jarrold, Phys. Rev. Lett. **91**, 215508 (2003).
⁹ G. A. Breaux, D. A. Hillman, C. M. Neal, R. C. Benirschke, and M. F. Jarrold, J. Am. Chem. Soc. **126**, 8682 (2004).
¹⁰ G. A. Breaux, C. M. Neal, B. Cao and M.F. Jarrold, Phys. Rev. Lett. **94**, 173401 (2005).
¹¹ G.A. Breaux, C. M. Neal, B. Cao and M.F. Jarrold, Phys. Rev. B **71**, 073410 (2005).
¹² S. Chacko, Kavita Joshi, D.G. Kanhere and S. A. Blundell, Phys. Rev. Lett. **92**, 135506 (2004).
¹³ K. Joshi, D. G. Kanhere and S.A. Blundell, Phys. Rev. B **66**, 155329 (2002).
¹⁴ K. Joshi, D. G. Kanhere and S.A. Blundell, Phys. Rev. B **67**, 235413 (2003).
¹⁵ F.-C. Chuang, C.Z. Wang, S.Ogut, J.R. Chelikowsky and K.M. Ho, Phys. Rev. B **69**, 165408 (2004).
¹⁶ K.Manninen, A. Rytönen and M. Manninen, Eur. Phys. J. **29**, 39 (2004).
¹⁷ S. Chacko, D.G. Kanhere and S. A. Blundell, Phys. Rev. B **71**, 155407 (2005).
¹⁸ Mal-Soon Lee, S. Chacko and D.G. Kanhere, *in communication*.
¹⁹ A. M. Ferrenberg and R. H. Swendsen, Phys. Rev. Lett. **61**, 2635 (1988); P. Labastie and R. L. Whetten, Phys. Rev. Lett. **65**, 1567 (1990).
²⁰ D. G. Kanhere, A. Vichare and S. A. Blundell, *Reviews in Modern Quantum Chemistry*, Edited by K. D. Sen, World Scientific, Singapore (2001).
²¹ E. A. Mason and E. W. McDaniel, Transport Properties of Ions in Gases, (Wiley, New York, 1988).
²² M.C. Payne, M.P. Teter, D.C. Allen, T.A. Arias, and J. D. Joannopoulos, Rev. Mod. Phys. **64**, 1045 (1992).
²³ D. Vanderbilt, Phys. Rev. B **41**, 7892 (1990).
²⁴ Vienna *Ab initio* simulation package, Technische Universität Wien (1999); G. Kresse and J. Furthmüller, Phys. Rev. B **54**, 11169 (1996).
²⁵ In our earlier work on gallium clusters [see Ref. 12], we have verified that the *d*-electrons do not significantly af-

fect the equilibrium geometries and the finite-temperature behavior.

²⁶ A. Vichare, D. G. Kanhere, and S. A. Blundell, *Phys. Rev. B* **64**, 045408 (2001).

²⁷ A typical bond-distance of a metallic bond seen in the extended system, *i.e.* α -gallium, is about 2.79 Å.

²⁸ The co-ordination number is computed by counting the number of atom lying within a sphere of radius of 2.79 Å. The radius 2.79 Å is chosen since this value corresponds to

the maximum bond-length of a metallic bond in the α -Ga bulk phase. For a description of α -Ga see, for instance, X. G. Gong, X. G. Gong, G. L. Chiarotti, M. Parrinello, and E. Tosatti, *Phys. Rev. B* **43**, 14277 (1991); V. Heine, *J. Phys. C* **1**, 222 (1968); V. Heine and D. Weaire, *Solid State Phys.* **24**, 249 (1970).

²⁹ B. Silvi, and A. Savin, *Nature (London)* **371**, 683 (1994).